J. Appl. Cryst. (1993). **26**, 706–716

Angle Calculations for a Six-Circle Surface X-ray Diffractometer

BY MARTIN LOHMEIER AND ELIAS VLIEG

FOM Institute for Atomic and Molecular Physics, Kruislaan 407, 1098 *SJ Amsterdam, The Netherlands*

(*Received* 7 *January* 1993; *accepted* 14 *May* 1993)

Abstract

Angle calculations are presented for a new type of diffractometer suitable for surface X-ray diffraction. The new geometry results from combining the four-circle and the *z*-axis geometries and involves six circles. Instruments based on this concept can be operated in different diffraction geometries. Compared to the four-circle and *z*-axis geometries, a larger fraction of the reciprocal space perpendicular to the sample is available to experiments when all six circles are used. This results in an improved out-of-plane resolution in any X-ray structure study. In each geometry, either the angle of incidence or the outgoing angle of the X-rays can be chosen. At the same time, the surface normal can be aligned in the horizontal diffractometer plane, providing optimum resolution and sample illumination. All equations are given in closed form. The different modes of operation are compared and operation schemes are discussed.

1. Introduction

The study of single-crystal surfaces by X-ray diffraction in recent years has resulted in the evolution of several types of diffractometers, employing different diffraction geometries (Feidenhans'l, 1989).

Many of the constructions go back to the four-circle normal-beam-geometry machine, worked out thoroughly by Busing & Levy (1967). This basically consists of three sample circles and one detector circle. While this type of diffractometer is well suited to bulk crystallography, it lacks the flexibility to deal with the specific boundary conditions required in surface X-ray diffraction, the most important of these being control over the X-ray angle of incidence on the sample, β_{in}, and the outgoing angle, β_{out}. In order to increase the surface sensitivity, one works at either grazing angles of incidence or small outgoing angles. A small angle of incidence results in low penetration depths and thus in low background levels from thermal diffuse or fluorescent bulk scattering. Small outgoing angles similarly result in low background levels because the outgoing beam can only emerge from the close vicinity of the surface. Small outgoing angles also yield high in-plane resolution if the detector slits are aligned with diffraction rods of the sample.

In addition, both the incoming and outgoing angles can be set close to the critical angle β_c, at which total external reflection can enhance the reflected intensities by a factor of four. Thus, in order to avoid intensity variations related to refraction, β_{in} and β_{out} have to be fixed or have to be sufficiently large compared with β_c.

The four-circle diffractometer allows the setting of β_{in} and β_{out}, for which useful procedures have been given by Mochrie (1988) and Robinson (1988*a*). However, this can only be accomplished by tilting the sample, which leads to undesirable correction factors caused by the changing resolution of the incoming beam incident on the tilted sample (Robinson, 1988*b*).

This difficulty is overcome by the five-circle type of diffractometer (Gibbs, Ocko, Zehner & Mochrie, 1990), for which Vlieg, Van der Veen, Macdonald & Miller (1987) have given angle calculations. This instrument is based on the four-circle type but features an additional rotary table on which the whole setup, including the sample and the detector, rests. The additional degree of freedom is used to align the surface normal in the horizontal diffractometer plane, which avoids complicated resolution corrections and guarantees maximum sample illumination.

A generally different approach has been undertaken by Brennan & Eisenberger (1984). By redistributing the four degrees of freedom on two detector and two sample circles in the so-called *z*-axis geometry, one obtains a diffractometer with two circles directly set to β_{in} and β_{out}. In principle, this allows for a larger perpendicular momentum transfer $q_\perp$ than does a five-circle instrument, resulting in better positional resolution in structure studies perpendicular to the sample surface (Vlieg, Robinson & Kern, 1990). The required angle settings for the *z*-axis geometry have been calculated by Bloch (1985). While this concept is intuitively attractive for surface X-ray diffraction, it has the disadvantage that the sample surface normal has to be aligned with the diffractometer axis. This makes an additional sample-tilt stage necessary, whose settings are fixed once the sample is aligned. The horizontal alignment gives the same benefits as

ISSN 0021-8898

discussed for the five-circle case. One further advantage of the z-axis geometry is that so-called ω scans (Stout & Jensen, 1968) can be performed by rotating only the ω circle. These types of scans are frequently used in surface X-ray structure determinations and are, in the four- and five-circle geometries, only approached by φ scans. The differences, however, are often negligible for practical cases. Typically, the ω axis is also more accurate than the (usually) smaller φ axis.

By combining the five-circle and z-axis characteristics into a six-circle instrument, one eliminates the disadvantages of the particular modes (extra tilt stage or limited perpendicular momentum transfer) and obtains a more flexible instrument. The six-circle diffractometer can equivalently be considered as a five-circle instrument with an additional out-of-plane detector arm or as a z-axis machine with a complete two-circle sample goniometer. Six-circle instruments are being constructed at several laboratories, for example, at the European Synchrotron Radiation Facility (ESRF, Grenoble, France) (Ferrer, 1992) and at the Photon Factory (Tsukuba, Japan) (Takahashi, Nakatani, Takahashi, Zhang & Ando, 1993).

In this paper, we present closed-form equations for the angle settings of a six-circle diffractometer for a given reflection (hkl) under the boundary conditions specified above, *i.e.* for either a fixed incoming angle or a fixed outgoing angle and for the horizontal-surface-normal condition. By taking full advantage of the two extra sample circles that are necessary in comparison with the z-axis machine, the instrument can be operated in various geometries. In addition to incorporating all previously mentioned advantages of the different types of diffractometers, the six-circle diffractometer features a larger accessible $q_\perp$ range compared with the four-circle and z-axis geometries for the important boundary conditions of work at either small incoming or small outgoing angles.

The paper is structured as follows. §2 describes the different circles of the diffractometer and treats the different geometries in which the instrument can be used. §3 is dedicated to transformations between different coordinate frames, which are used for the calculation of the angle settings. In §4, all the basic equations that govern the angle settings are derived. The setting of the detector angle δ is independent of the geometry used and is derived in §5. All the remaining angle settings in the z-axis mode are given in §6. §7 deals with the corresponding angle settings in the five-circle geometry. In §8, the different geometries are compared. Concepts for using the diffractometer are discussed and the increase in the available reciprocal-space fraction in the six-circle geometry is demonstrated. Finally, a mirror image of the instrument is described in the Appendix.

All equations are given in matrix form, where this is useful, in order to allow for straightforward numerical implementation. All the procedures described below have been thoroughly numerically tested* and have been successfully implemented in the control program of the six-circle diffractometer at ESRF, *SPEC* (Certified Scientific Software, 1992).

2. The six-circle diffractometer

2.1. *Definition*

The present six-circle diffractometer is based on the five-circle diffractometer layout given by Gibbs *et al.* (1990). The five-circle type is extended by an additional γ circle, which facilitates out-of-plane positioning of the detector. There are six degrees of freedom in total, which can be subdivided into one shared, two detector and three sample degrees of freedom.

The diffractometer is shown with all angles set to zero in Fig. 1 and with all angles having values in the first quadrant in Fig. 2. The laboratory-frame coordinates x, y and z are chosen such that, with all angles set to zero, the horizontal diffractometer plane lies in the yz plane, the X-ray beam impinges on the sample along the positive-y direction and the φ axis points along the positive-z direction. Note that this is the convention used by Busing & Levy (1967) but in our case the z axis is horizontal whereas their z axis was vertical. This orientation has no effect on the outcome of the angle calculations.

The sample is mounted on the φ axis, which can rotate about the χ axis. Both the χ and φ circles

*Suitable computer code is available on request from the authors.

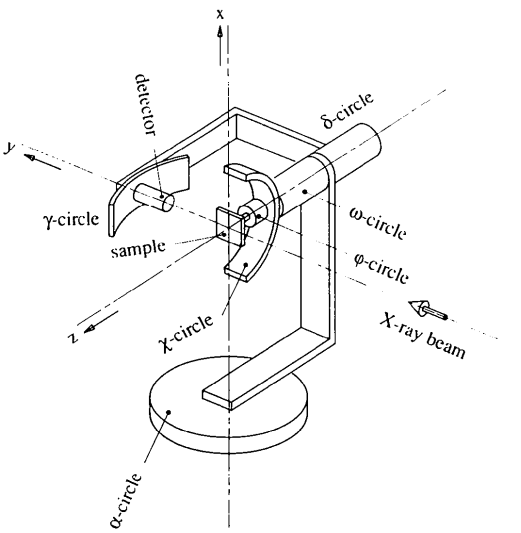

Fig. 1. A schematic drawing of the six-circle diffractometer with all circles set to the zero position.

are supported by the ω circle, which rests on the main diffractometer mount. The detector is mounted on the γ circle, which is fixed to the detector arm. The latter can rotate about the δ axis, which coincides with the ω axis. The whole setup is mounted on top of a rotary table, which gives the sixth degree of freedom about the α axis.

The ω zero position is chosen to agree with the convention used by Busing & Levy (1967) and is thus different from the one used by Vlieg *et al.* (1987).

2.2. *Modes of operation*

With six degrees of freedom, the diffractometer can operate in different geometries, which we call operation modes. In a diffraction experiment, one has to fulfil the general diffraction condition, *i.e.* the momentum transfer vector **Q** must match a point (*hkl*) in reciprocal space. This consumes three degrees of freedom. A fourth degree of freedom is used to work at either a fixed incoming angle β_{in} or a fixed outgoing angle β_{out}, or to work under the $\beta_{in} = \beta_{out}$ condition. We do not discuss the case where β_{in} and β_{out} are fixed simultaneously because then $q_\perp$ cannot be specified. The fifth boundary condition is used to keep the surface normal in the horizontal plane. This leaves an ambiguity with respect to the last degree of freedom, which can be resolved by fixing one or more of the diffractometer angles to a given value.

We distinguish between the following modes of operation (see also Table 1).

z-axis mode. In this mode, the sample circles χ and φ are fixed such that the surface normal lies in the horizontal plane and coincides with the diffractometer ω axis. The other four circles (α, δ, γ, ω) are used to satisfy the diffraction equation and one of the three β conditions. Thus, in this mode, all six degrees of freedom are used.

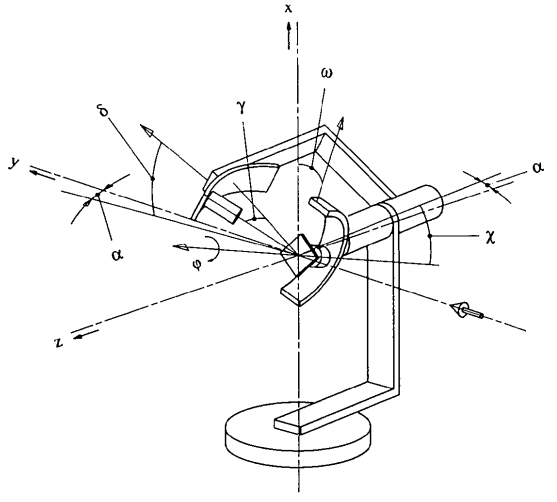

Fig. 2. The diffractometer with all circles having a setting in the first quadrant.

Table 1. *Distribution of the boundary conditions over the six degrees of freedom*

In each geometry, the values of three angles are set to fulfil the diffraction condition and a fourth angle is fixed by one of the β conditions, leaving two remaining degrees of freedom to distinguish between the modes of operation.

Mode of operation	Fixed angles α	γ	χ	φ	Surface normal horizontal
z axis			√*	√*	√
Five circle/γ		√†			√
Five circle/α	√†				√
Four circle	√†	√†			
Six circle	α_{max}‡	γ_{max}‡			√

* Value given by alignment of surface normal with ω axis.
† Set to any required value.
‡ Depending on which limit is met, either α or γ is set to its maximum value.

Five-circle mode. Either γ or α is fixed and the values of the remaining five angles are obtained from the diffraction condition, one of the β conditions and the surface-normal condition. If γ is set to zero, this mode is identical with the mode given by Vlieg *et al.* (1987). Setting γ to nonzero values allows the accessing of larger $q_\perp$ values, as is discussed in §8.

Four-circle mode. This mode is identical to the five-circle mode except that the condition of the surface normal is given up. Both α and γ are fixed to given values.

In addition to these modes, we introduce the so-called six-circle mode. This mode is identical to the z-axis mode until either α or γ exceed their limit values. In these cases, α or γ is set to its limit value and the remaining five circles are calculated in the five-circle mode. An important extension of the z-axis mode is hereby achieved. Whereas φ and χ are fixed in the z-axis mode, now the full ranges of φ and χ are utilized. This effectively increases the available $q_\perp$ range, as is shown below.

3. Coordinate transformations

In order to derive convenient expressions for the diffraction and boundary conditions, it is necessary to work in different coordinate frames attached to the different circles and to be able to transform equations between these frames.

Reciprocal-space coordinates are written as

$$\mathbf{H} = h\mathbf{b}_1 + k\mathbf{b}_2 + l\mathbf{b}_3, \tag{1}$$

where the $\mathbf{b}_i$ denote reciprocal-lattice vectors, which are related to the real lattice vectors $\mathbf{a}_i$ by

$$\mathbf{a}_i \cdot \mathbf{b}_j = 2\pi\delta_{i,j}. \tag{2}$$

The transformation of $\mathbf{H}$ into laboratory-frame coordinates $\mathbf{H}_{\rm lab}$ or into a coordinate frame fixed to a detector circle can be envisaged in three steps. First, $\mathbf{H}$ is converted into a Cartesian coordinate frame vector $\mathbf{H}_{\rm Cart}$ by a matrix B:

$$\mathbf{H}_{\rm Cart} = B\mathbf{H}. \tag{3}$$

We choose a Cartesian frame $(\mathbf{e}_x, \mathbf{e}_y, \mathbf{e}_z)$ such that $\mathbf{e}_x$ is parallel to $\mathbf{b}_1$, $\mathbf{e}_y$ lies in the plane of $\mathbf{b}_1$ and $\mathbf{b}_2$ and $\mathbf{e}_z$ is perpendicular to that plane. The matrix B contains all lattice parameters of the sample. It has been given by Busing & Levy (1967) for our particular choice of $(\mathbf{e}_x, \mathbf{e}_y, \mathbf{e}_z)$ in the form

$$B = \begin{bmatrix} b_1 & b_2\cos\beta_3 & b_3\cos\beta_2 \\ 0 & b_2\sin\beta_3 & -b_3\sin\beta_2\cos\alpha_1 \\ 0 & 0 & 1/a_3 \end{bmatrix}. \tag{4}$$

The second step is to establish the orientational relationship between the Cartesian coordinate system and the diffractometer φ axis. This can be described by the orientation matrix U:

$$\mathbf{H}_\varphi = U\mathbf{H}_{\rm Cart}. \tag{5}$$

In the third step, one can attach Cartesian coordinate frames to each of the six diffractometer axes. The transformation of $\mathbf{H}_\varphi$ into these frames is accomplished by successive application of the following rotation matrices, which can easily be derived from Fig. 2:

$$A = \begin{bmatrix} 1 & 0 & 0 \\ 0 & \cos\alpha & -\sin\alpha \\ 0 & \sin\alpha & \cos\alpha \end{bmatrix}; \quad \Delta = \begin{bmatrix} \cos\delta & \sin\delta & 0 \\ -\sin\delta & \cos\delta & 0 \\ 0 & 0 & 1 \end{bmatrix};$$
$$\Gamma = \begin{bmatrix} 1 & 0 & 0 \\ 0 & \cos\gamma & -\sin\gamma \\ 0 & \sin\gamma & \cos\gamma \end{bmatrix}; \quad \Omega = \begin{bmatrix} \cos\omega & \sin\omega & 0 \\ -\sin\omega & \cos\omega & 0 \\ 0 & 0 & 1 \end{bmatrix};$$
$$X = \begin{bmatrix} \cos\chi & 0 & \sin\chi \\ 0 & 1 & 0 \\ -\sin\chi & 0 & \cos\chi \end{bmatrix}; \quad \Phi = \begin{bmatrix} \cos\varphi & \sin\varphi & 0 \\ -\sin\varphi & \cos\varphi & 0 \\ 0 & 0 & 1 \end{bmatrix}. \tag{6}$$

By this convention, Φ transforms a vector from the φ-axis frame into the χ-axis frame, X transforms this vector into the ω-axis frame *etc*:

$$\mathbf{H}_\varphi \xrightarrow{\Phi} \mathbf{H}_\chi \xrightarrow{X} \mathbf{H}_\omega \xrightarrow{\Omega} \mathbf{H}_\alpha \xrightarrow{A} \mathbf{H}_{\rm lab} \xrightarrow{A^{-1}} \mathbf{H}_\alpha \xrightarrow{\Delta^{-1}} \mathbf{H}_\delta \xrightarrow{\Gamma^{-1}} \mathbf{H}_\gamma.$$

4. Basic equations

In the following, we derive the basic equations that determine the settings of all six diffractometer circles for a given reflection (hkl) and either a fixed angle of incidence $\beta_{\rm in}$ or a fixed outgoing angle $\beta_{\rm out}$ and the horizontal-surface-normal condition.

4.1. *The diffraction equation*

For constructive interference between diffracted beams to occur, the momentum transfer vector $\mathbf{Q} \equiv \mathbf{K}_f - \mathbf{K}_i$ must match a reciprocal-lattice vector $\mathbf{H} = h\mathbf{b}_1 + k\mathbf{b}_2 + l\mathbf{b}_3$:

$$\mathbf{H} = \mathbf{K}_f - \mathbf{K}_i, \tag{7}$$

where $\mathbf{K}_i$ and $\mathbf{K}_f$ are the momentum vectors of the incoming and outgoing X-rays, respectively.

In bulk diffraction, Bragg peaks occur if h, k and l are all integers whereas, in surface X-ray diffraction, h and k can have fractional values because of surface reconstruction (larger surface unit cell) and l may assume any value because of the absence of periodicity perpendicular to the surface.* In order to scan peak profiles or diffuse intensity distributions, we must allow h, k and l to have any real values.

Equation (7) can be evaluated in any coordinate frame. However, it is convenient to do this in the α-axis frame. The incoming-beam vector $\mathbf{K}_{i,\rm lab} = (0, K, 0)$ points along the y direction of the laboratory frame and the A^{-1} matrix transforms this vector into the α-axis frame:

$$\mathbf{K}_{i,\alpha} = A^{-1}\mathbf{K}_{i,\rm lab}. \tag{8}$$

The length of $\mathbf{K}_i$ is given by $K = 2\pi/\lambda$, where λ is the wavelength of the incoming X-rays.

The outgoing-beam vector points along the direction of the detector-frame y axis and has the same length, K. It can thus be written as

$$\mathbf{K}_{f,\alpha} = \Delta\Gamma\mathbf{K}_{i,\rm lab}. \tag{9}$$

Finally, the reciprocal-lattice vector $\mathbf{H}$ is, in the α-axis frame, given by

$$\mathbf{H}_\alpha = \Omega X \Phi U B \mathbf{H}. \tag{10}$$

Substituting (8), (9) and (10) into (7), one obtains

$$\Omega X \Phi U B \mathbf{H} = (\Delta\Gamma - A^{-1})\mathbf{K}_{i,\rm lab}, \tag{11}$$

which is the basic diffraction equation for the six-circle diffractometer. Equation (11) couples all six angles of the diffractometer to the reciprocal-space coordinates (hkl).

Procedures for finding the elements of U rely on (11), written in the form

$$UB\mathbf{H} = \mathbf{Q}_\varphi, \tag{12}$$

* In surface X-ray diffraction, the low-energy electron diffraction (LEED) convention is most often followed, in which h and k are in the surface plane and l denotes the direction perpendicular to the surface. It is not necessary to follow this convention, but choosing a different unit cell leads in general to a more complicated indexing of reciprocal space. For simplicity, l is used here to denote the direction perpendicular to the surface. The angle calculations as presented in the following, however, are not based on this assumption.

with

$$\mathbf{Q}_\varphi = \Phi^{-1}X^{-1}\Omega^{-1}(\Delta\Gamma - A^{-1})\mathbf{K}_{i,\text{lab}}. \quad (13)$$

Suitable recipes have been given by Busing & Levy (1967).

4.2. *Definition of incoming and outgoing angles*

In order to describe the angle between the incoming beam and the sample surface, β_{in}, and the corresponding angle of the outgoing beam, β_{out}, we define the surface normal as the vector perpendicular to the optical sample surface. To account for the difference between the z axis of the φ-axis frame and the optical surface normal, two angles σ and τ are introduced. The corresponding matrices are

$$\Sigma = \begin{bmatrix} \cos\sigma & 0 & \sin\sigma \\ 0 & 1 & 0 \\ -\sin\sigma & 0 & \cos\sigma \end{bmatrix};$$
$$T = \begin{bmatrix} \cos\tau & \sin\tau & 0 \\ -\sin\tau & \cos\tau & 0 \\ 0 & 0 & 1 \end{bmatrix}. \quad (14)$$

The deviation of the optical surface normal (described by Σ and T) from the crystallographic orientation (described by UB) is equivalent to the sample miscut. The values of the two angles σ and τ can be found by observing the reflection of a laser light source from the sample. The values of $-\chi$ and $-\varphi$ are σ and τ, respectively, if the reflected spot does not move under ω rotations.

The angle of incidence β_{in} is defined as the angle between the incoming beam and its projection on the optical surface. This can be expressed in the α-axis frame by the scalar product of the surface normal (equivalent to the z axis in the sample frame) and the incoming beam (pointing along the y axis in the laboratory frame):

$$\Omega X\Phi S\begin{bmatrix}0\\0\\1\end{bmatrix} A^{-1}\begin{bmatrix}0\\1\\0\end{bmatrix} = -\sin\beta_{in}, \quad (15)$$

where $S = T\Sigma$.

Equivalently, the outgoing angle β_{out} is defined as the angle between the outgoing beam and its projection on the optical surface by

$$\Omega X\Phi S\begin{bmatrix}0\\0\\1\end{bmatrix} \Delta\Gamma\begin{bmatrix}0\\1\\0\end{bmatrix} = \sin\beta_{out}. \quad (16)$$

β_{in} and β_{out} cannot be selected independently but are coupled by the momentum transfer perpendicular to the surface. Writing (11) as

$$\Delta\Gamma\begin{bmatrix}0\\1\\0\end{bmatrix} = \Omega X\Phi UB(\mathbf{H}/K) + A^{-1}\begin{bmatrix}0\\1\\0\end{bmatrix}, \quad (17)$$

substituting this into (16),

$$\Omega X\Phi S\begin{bmatrix}0\\0\\1\end{bmatrix}\left(\Omega X\Phi UB(\mathbf{H}/K) + A^{-1}\begin{bmatrix}0\\1\\0\end{bmatrix}\right) = \sin\beta_{out}, \quad (18)$$

and combining this with (15), one gets

$$\begin{bmatrix}0\\0\\1\end{bmatrix}[S^{-1}UB(\mathbf{H}/K)] - \sin\beta_{in} = \sin\beta_{out} \quad (19)$$

or

$$\sin\beta_{in} + \sin\beta_{out} = (1/K)(S^{-1}UB\mathbf{H})_3. \quad (20)$$

This equation can be used for calculating β_{in} from β_{out} or *vice versa*, if the momentum-transfer vector $\mathbf{H}$ is given. This means that one generally has to choose between the following useful boundary conditions:

(i) β_{in} fixed;
(ii) β_{out} fixed;
(iii) $\beta_{in} = \beta_{out}$.

4.3. *Horizontal surface normal*

It is important to have the sample oriented with its surface normal horizontal (*i.e.* in the laboratory yz plane) for two reasons. First, it leads to a well defined illuminated surface area, which is close to the central part of the beam, *i.e.* receives the highest flux. Second, it avoids complicated resolution corrections in scans with large $q_\perp$, which would otherwise be necessary due to tilting of the sample with respect to the incoming beam (Robinson, 1988*b*). In general, the calculation of resolution effects is very complicated and is strongly dependent on the experimental geometry chosen. For example, for a focused synchrotron beam line, the divergence in the horizontal plane is much larger than in the vertical plane. By aligning the surface normal with the horizontal plane, the surface diffraction rod is aligned with the large divergence direction of the beam. This leads to maximum in-plane resolution and maximum peak intensity if β_{out} is kept small.

The horizontal-surface-normal condition can be written in the α-axis frame as

$$\Omega X\Phi S\begin{bmatrix}0\\0\\1\end{bmatrix} A^{-1}\begin{bmatrix}1\\0\\0\end{bmatrix} = 0. \quad (21)$$

5. Detector angle δ

The first angle to be calculated is the detector angle δ because this can be done regardless of the mode of operation of the diffractometer. Equation (11) can be written as $\mathbf{H}_\alpha = \mathbf{Q}_\alpha$. The lengths of these vectors have to be equal. Since Ω, X and Φ are unitary, this gives

$$\mathbf{H}_\varphi^2 = \mathbf{H}_\alpha^2 = |(A\Gamma - A^{-1})\mathbf{K}_{i,\mathrm{lab}}|^2. \tag{22}$$

This can be evaluated as

$$\mathbf{H}_\varphi^2 = 2K^2(1 - \cos\delta\cos\gamma\cos\alpha + \sin\gamma\sin\alpha) \tag{23}$$

or

$$\delta = \arccos\{[1 - \mathbf{H}_\varphi^2/(2K^2) + \sin\gamma\sin\alpha] \times [\cos\gamma\cos\alpha]^{-1}\}. \tag{24}$$

Given the reflection $\mathbf{H} = hkl$, the settings of the rotary table α and the out-of-plane detector angle γ, one can calculate δ from (24). Note, however, that α and γ will depend on the operation mode.

The scattering angle, 2θ, can now be calculated as follows:

$$\cos 2\theta = \mathbf{K}_f \cdot \mathbf{K}_i/K^2 = A\Delta\Gamma \begin{bmatrix} 0 \\ 1 \\ 0 \end{bmatrix} \begin{bmatrix} 0 \\ 1 \\ 0 \end{bmatrix} \tag{25}$$

or

$$\cos 2\theta = \cos\alpha\cos\gamma\cos\delta - \sin\alpha\sin\gamma. \tag{26}$$

For $\alpha = \gamma = 0$, one obtains a four-circle diffractometer and (26) reduces to $2\theta = \delta$. Combining (24) and (26), one obtains*

$$\cos 2\theta = 1 - (\mathbf{H}_\varphi^2/2K^2), \tag{27}$$

from which follows

$$2\sin\theta = |\mathbf{H}|/K, \tag{28}$$

which is Bragg's law, if one writes $|H| = 2\pi n/d$, where d is the distance between two lattice planes and n is an integer.

6. Angle settings in the z-axis mode

In the z-axis mode, one aligns the optical surface normal with the diffractometer ω axis by fixing φ and χ at

$$\varphi = -\tau, \tag{29a}$$

$$\chi = -\sigma. \tag{29b}$$

With these settings, the surface normal lies in the horizontal diffractometer plane, *i.e.* (21) is satisfied. The settings of the remaining four circles can easily be found by rewriting (11) in the ω-axis frame:

$$\mathbf{H}_\omega = X\Phi UB\mathbf{H} = \Omega^{-1}(A\Gamma - A^{-1})\mathbf{K}_{i,\mathrm{lab}} \tag{30}$$

or, written in components:

$$(1/K)\begin{bmatrix} H_{\omega,1} \\ H_{\omega,2} \\ H_{\omega,3} \end{bmatrix} = \begin{bmatrix} \cos\omega\sin\delta\cos\gamma - \sin\omega(\cos\delta\cos\gamma + \cos\alpha) \\ \sin\omega\sin\delta\cos\gamma + \cos\omega(\cos\delta\cos\gamma - \cos\alpha) \\ \sin\gamma + \sin\alpha \end{bmatrix}. \tag{31}$$

From the z component of the last equation, the values of α and γ can be obtained, depending on whether β_{in} or β_{out} is fixed or $\beta_{\mathrm{in}} = \beta_{\mathrm{out}}$:

β_{in} fixed: $\alpha = \beta_{\mathrm{in}}$,

$$\gamma = \beta_{\mathrm{out}} = \arcsin[(H_{\omega,3}/K) - \sin\beta_{\mathrm{in}}]; \tag{32a}$$

β_{out} fixed: $\gamma = \beta_{\mathrm{out}}$,

$$\alpha = \beta_{\mathrm{in}} = \arcsin[(H_{\omega,3}/K) - \sin\beta_{\mathrm{out}}]; \tag{32b}$$

$\beta_{\mathrm{in}} = \beta_{\mathrm{out}}$: $\alpha = \gamma = \beta_{\mathrm{in}} = \beta_{\mathrm{out}} = \arcsin(H_{\omega,3}/2K)$. (32c)

Note that, in all three cases, α equals the angle of incidence β_{in} and γ equals the outgoing angle β_{out}.

The x and y components of (31) can be used to derive an expression for ω:*

$$\omega = \arctan[H_{\omega,2}\sin\delta\cos\gamma - H_{\omega,1}(\cos\delta\cos\gamma - \cos\alpha), H_{\omega,1}\sin\delta\cos\gamma + H_{\omega,2}(\cos\delta\cos\gamma - \cos\alpha)] \tag{33}$$

The setting of the detector-arm angle δ has already been given in §5.

7. Angle settings in the five- and four-circle modes

In the five-circle mode, either α or γ is fixed and the remaining angle γ or α is set to satisfy the horizontal-surface-normal condition. In the four-circle mode, both α and γ can be set to fixed values, but the horizontal-surface-normal condition has to be given up.

The calculation of the remaining four circles in the form given below requires the knowledge of the angle of incidence β_{in}. In cases where one wants to fix β_{out} instead, or work with the $\beta_{\mathrm{in}} = \beta_{\mathrm{out}}$ condition, one can use (20) to calculate β_{in}.

First, procedures for the calculation of γ and α are presented, followed by calculation schemes for the corresponding settings of ω, χ and φ.

* For numerical evaluation of ω, the four-quadrant two-argument arctan function, as implemented in many modern compilers, should be used. We simply refer to this function as the arctan function subsequently.

7.1. *Settings of the rotary table α and out-of-plane angle γ*

Combining the horizontal-surface-normal condition (21) and the angle of incidence, given by (15), in the laboratory frame, and writing them in vector notation, one obtains

$$YS\begin{bmatrix}0\\0\\1\end{bmatrix}=\begin{bmatrix}0\\-\sin\beta_{in}\\\cos\beta_{in}\end{bmatrix}, \tag{34}$$

where Y is defined by

$$Y = A\Omega X\Phi. \tag{35}$$

The unitary matrix Y transforms the vector on the left-hand side of (34) into the one on the right-hand side. From (34), one cannot uniquely calculate Y because an initial rotation about (0, 0, 1) or a final rotation about $(0, -\sin\beta_{in}, \cos\beta_{in})$ would result in the same transformation. However, one can absorb this ambiguity into a single rotation angle v if Y is written as

$$Y = Z^{-1}NZY_0, \tag{36}$$

where Y_0 is a particular solution of (34). Construction of such a particular solution is easily accomplished and a suitable recipe has been given in Vlieg *et al.* (1987). Z is given by

$$Z=\begin{bmatrix}1&0&0\\0&\cos\beta_{in}&\sin\beta_{in}\\0&-\sin\beta_{in}&\cos\beta_{in}\end{bmatrix} \tag{37}$$

and N is defined as

$$N=\begin{bmatrix}\cos v&\sin v&0\\-\sin v&\cos v&0\\0&0&1\end{bmatrix}. \tag{38}$$

The angle v can be found using the general diffraction equation (11). Defining

$$\mathbf{H}_v = ZY_0UB\mathbf{H}, \tag{39}$$

one derives

$$\underbrace{Z^{-1}N(\mathbf{H}_v/K)}_{=:\mathbf{v}} = \underbrace{(A\Delta\Gamma - I)\begin{bmatrix}0\\1\\0\end{bmatrix}}_{=:\mathbf{w}}. \tag{40}$$

Note that $\mathbf{H}_v$ can be directly evaluated from (39) and is independent of v.

With substitution for $\cos\delta$ using (24) and (27), (40) becomes

$$\left(\frac{1}{K}\right)\begin{bmatrix}H_{v,1}\cos v + H_{v,2}\sin v\\(H_{v,2}\cos v - H_{v,1}\sin v)\cos\beta_{in} - H_{v,3}\sin\beta_{in}\\(H_{v,2}\cos v - H_{v,1}\sin v)\sin\beta_{in} + H_{v,3}\cos\beta_{in}\end{bmatrix}$$
$$=\begin{bmatrix}\sin\delta\cos\gamma\\\cos 2\theta - 1\\\tan\alpha\cos 2\theta + \sin\gamma/\cos\alpha\end{bmatrix}. \tag{41}$$

v can be eliminated by combining the y and z components of (41) in the form

$$(v_2 - w_2)\sin\beta_{in} - (v_3 - w_3)\cos\beta_{in} = 0. \tag{42}$$

One obtains

$$\underbrace{[(1-\cos 2\theta)\sin\beta_{in} - (H_{v,3}/k)]}_{=:a}\cos\alpha + \underbrace{\cos 2\theta\cos\beta_{in}}_{=:b}\sin\alpha = \underbrace{-\cos\beta_{in}\sin\gamma}_{=:c}. \tag{43}$$

Solving for α, one obtains

$$\alpha = 2\arctan[b \pm (b^2 + a^2 - c^2)^{1/2}, a + c]. \tag{44}$$

Alternatively, one can solve (43) for γ:

$$\gamma = -\arcsin\{\cos 2\theta\sin\alpha + [\tan\beta_{in}(1-\cos 2\theta) - (1/\cos\beta_{in})(H_{v,3}/K)]\cos\alpha\}. \tag{45}$$

Thus, from (44), α can be calculated for a given γ such that the surface normal is horizontal. Alternatively, (45) gives the corresponding value of γ for a given α.

7.2. *Settings of the sample circles ω, χ and φ*

In order to find the settings of the remaining three circles, the diffraction condition (11) is written in the form

$$R\mathbf{H}_\varphi = \mathbf{Q}_\alpha, \tag{46}$$

where $\mathbf{H}_\varphi = UB\mathbf{H}$ and

$$\mathbf{Q}_\alpha = (A\Delta\Gamma - A^{-1})\mathbf{K}_{i,lab} \tag{47}$$

is the momentum-transfer vector in the α-axis frame and the R matrix is defined as

$$R = \Omega X\Phi. \tag{48}$$

In order to derive the elements of the matrix R, a trick similar to that of the preceding section can be used by writing

$$R = D^{-1}\Psi DR_0, \tag{49}$$

where R_0 is a particular solution of (46). D is defined by

$$D(\mathbf{Q}_\alpha/Q_\alpha)=\begin{bmatrix}1\\0\\0\end{bmatrix} \tag{50}$$

and Ψ is given by

$$\Psi = \begin{bmatrix} 1 & 0 & 0 \\ 0 & \cos\psi & \sin\psi \\ 0 & -\sin\psi & \cos\psi \end{bmatrix}. \tag{51}$$

The value of ψ can be determined from the angle-of-incidence condition. If one writes (15) in the laboratory frame,

$$AD^{-1}\Psi DR_0 S \begin{bmatrix} 0 \\ 0 \\ 1 \end{bmatrix} \begin{bmatrix} 0 \\ 1 \\ 0 \end{bmatrix} = -\sin\beta_{\text{in}}, \tag{52}$$

and defines

$$V = AD^{-1} \tag{53}$$

and

$$\mathbf{u} = DR_0 S \begin{bmatrix} 0 \\ 0 \\ 1 \end{bmatrix}, \tag{54}$$

(52) becomes

$$\underbrace{(u_2 V_{2,2} + u_3 V_{2,3})}_{=:a} \cos\psi + \underbrace{(u_3 V_{2,2} - u_2 V_{2,3})}_{=:b} \sin\psi = \underbrace{\sin\beta_{\text{in}} - V_{2,1} u_1}_{=:c}, \tag{55}$$

which is of the same form as (43) and can be solved using (44).

ψ having been found, R can be evaluated using (49). Writing (48) in components [*cf.* Busing & Levy (1967)]:

$$R = \begin{bmatrix} \cos\omega\cos\chi\cos\varphi - \sin\omega\sin\varphi & \cos\omega\cos\chi\sin\varphi + \sin\omega\cos\varphi & \cos\omega\sin\chi \\ \sin\omega\cos\chi\cos\varphi - \cos\omega\sin\varphi & \cos\omega\cos\varphi - \sin\omega\cos\chi\sin\varphi & -\sin\omega\sin\chi \\ \sin\chi\cos\varphi & -\sin\chi\sin\varphi & \cos\chi \end{bmatrix}, \tag{56}$$

one obtains the settings of the three circles ω, χ and φ as

$$\omega = -\arctan[R_{23}, R_{13}] \tag{57}$$

$$\chi = \arcsin(R_{13}^2 + R_{23}^2)^{1/2} \tag{58}$$

$$\varphi = \arctan[-R_{32}, -R_{31}], \tag{59}$$

where the more obvious $\chi = \arccos(R_{33})$ has not been used for numerical reasons.

8. Discussion

Both the z-axis and five-circle modes can be used to measure diffraction intensities at a given set (h, k, l) while simultaneously satisfying one of the three β conditions and the horizontal-surface-normal condition. In practice, however, one encounters physical limits on some of the six circles, which necessitate the finding of an 'optimum mode' for a given scattering situation. The range of the χ circle, for instance, is typically restricted by the fact that the UHV chamber (which may be heavy and which can have many flanges holding other UHV equipment) is coupled to the χ circle by elastic bellows. Although *in situ* χ circles are currently not yet available, these will also have limited ranges owing to size/weight restrictions of the UHV chamber. Fitting the vacuum chamber directly to the χ circle, on the other hand, places severe weight limits on the vacuum chamber (Feidenhans'l, 1986), which compromises *in situ* X-ray measurements, for example, during sample preparation. For this reason, latest-generation surface X-ray diffractometers are mostly of the bellows type.

The effective ranges of both the α and γ circles are limited by the dimensions of the beryllium window through which the X-ray beams enter and leave the UHV chamber. Fitting beryllium windows to stainless-steel chambers is a rather delicate and expensive matter and thus cannot be done in arbitrarily large dimensions.

As pointed out in the *Introduction*, one of the most important boundary conditions in surface X-ray diffraction is to work at either grazing angles of incidence β_{in} – typically of the order of 1° – or small outgoing angles β_{out}. The three angles mentioned above (α, γ and χ) mainly affect the maximum perpendicular momentum transfer $q_\perp$ that can be reached by the diffractometer in the different modes. In the z-axis mode, this can be seen from (32), which gives the following limits for small incoming and small outgoing angles:

$$\begin{aligned} \beta_{\text{in}} \text{ small:} \quad q_{\perp,\varphi}^{\max}/K &= H_{\varphi,3}^{\max}/K \\ &\simeq H_{\omega,3}^{\max}/K \\ &= \sin\gamma_{\max} + \sin\beta_{\text{in}} \\ &\simeq \sin\gamma_{\max}; \end{aligned} \tag{60a}$$

$$\begin{aligned} \beta_{\text{out}} \text{ small:} \quad q_{\perp,\varphi}^{\max}/K &= H_{\varphi,3}^{\max}/K \\ &\simeq H_{\omega,3}^{\max}/K \\ &= \sin\alpha_{\max} + \sin\beta_{\text{out}} \\ &\simeq \sin\alpha_{\max}. \end{aligned} \tag{60b}$$

$H_{\varphi,3} \simeq H_{\omega,3}$ is exact if the orientation angle σ equals zero. In most cases, σ will be small enough to make this a good approximation.

In the five-circle mode, the following approximations hold:

$$\beta_{\text{in}} \simeq \alpha - \chi, \tag{61a}$$

$$\beta_{\text{out}} \simeq \gamma + \chi, \tag{61b}$$

from which, in combination with (20), the following restrictions can be derived:

$$\beta_{in} \text{ small:} \quad \chi \simeq \alpha,\ q_{\perp,\varphi}^{max}/K = H_{\varphi,3}^{max}/K \simeq \sin(\gamma^{max} + |\chi^{max}|); \tag{62a}$$

$$\beta_{out} \text{ small:} \quad \chi \simeq -\gamma,\ q_{\perp,\varphi}^{max}/K = H_{\varphi,3}^{max}/K \simeq \sin(\alpha^{max} + |\chi^{max}|). \tag{62b}$$

In the last approximation, use has been made of the fact that χ can assume positive as well as negative values.

One can now use (60) and (62) to characterize the different operation modes with respect to the accessible reciprocal-space region. The range available in the five-circle mode given by Vlieg *et al.* (1987) is obtained by taking $\gamma = 0$. In that case, $\chi \simeq 0$ for small β_{out}, leading to $q_{\perp,\varphi}^{max}/K \simeq \sin(\alpha^{max})$. The smallest range available is in this five-circle ($\gamma = 0$) mode, for small β_{in}. For small β_{out}, the range is approximately the same as for the z-axis geometry if $\alpha^{max} = \gamma^{max}$. Of course, one can reach larger $q_\perp$ in the z-axis mode, but only at the expense of having both β_{in} and β_{out} large. The six-circle geometry, on the other hand, allows for large $q_\perp$ and small β_{in} or β_{out} at the same time. As a numerical example, we discuss the case where $\alpha^{max} = \gamma^{max}$ and α^{max} and χ^{max} have typical values of 25 and 15°, respectively. Compared to the five-circle ($\gamma = 0$) mode at small β_{in}, with this geometry one gains an increase in available l space of about

(*a*) 60% when either working at small β_{out} in the $\gamma = 0$ mode or working in the z-axis mode with β_{in} or β_{out} small and

(*b*) 150% when working in the six-circle mode at either small β_{in} or small β_{out}.

In the z-axis geometry, the two weakest circles (χ and φ) are fixed. Therefore, there are mechanical advantages to working in the z-axis mode until one of the two limits of (60) is met. One can then set either α or γ to its maximum value and compute the corresponding angle γ or α as well as ω, χ and φ in the five-circle mode. Thus, by using χ and φ in the five-circle mode, with γ or α at its maximum value, it is possible to reach larger $q_\perp$ values than in the z-axis mode, where χ is fixed. This is illustrated in Fig. 3.

Instead of using a full γ circle, one might, for simplicity, even consider two independent detectors, positioned at $\gamma = 0$ and $\gamma = \gamma_{max}$. This will also make larger $q_\perp$ values accessible. The five-circle mode with an appropriate χ range will smoothly join the two detector positions. This option is currently being implemented at the surface X-ray diffractometer at Daresbury Laboratory, England (Norris, Taylor, Moore & Harris, 1987).

The five-circle mode offers one more possibility: as one of the six circles (α or γ) is fixed beforehand, one could use this last degree of freedom to optimize motor movements between two scans at different (h, k, l) values. Because all angle-determining equations are given in closed form, computation of the five angles is very fast, even on a simple PC, while circle rotation times consume a growing fraction of the

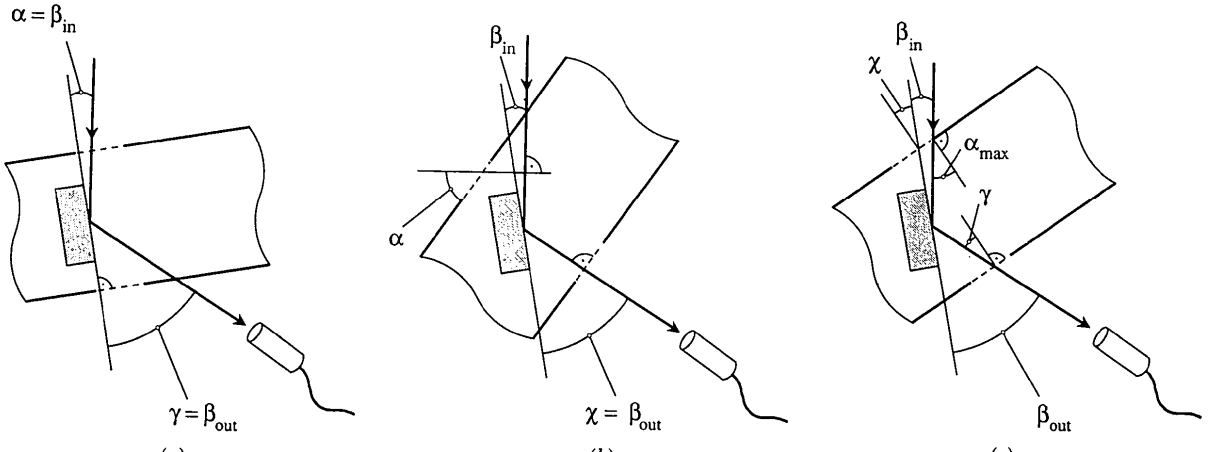

Fig. 3. Schematic top-plane view of the different geometries for the case of a large $q_\perp$, a small incoming angle β_{in} and a large outgoing angle β_{out}. The incoming and outgoing X-ray beams should pass through the beryllium windows (dashed lines), but may become obstructed by the UHV chamber (thick solid lines). The diffracting sample is drawn as a shaded block. (*a*) z-axis geometry. $\alpha = \beta_{in}$, $\gamma = \beta_{out}$. The outgoing beam is blocked. (*b*) Five-circle ($\gamma = 0$) geometry. Outgoing beam and UHV chamber are aligned, χ rotates the sample with respect to the chamber. The incoming beam is blocked. (*c*) Five-circle ($\gamma \neq 0$) geometry. α is set to its maximum value, such that the incoming beam is just not blocked by the chamber. γ and χ define the outgoing angle β_{out}. Note that the outgoing beam is also not blocked.

available beam time with the advent of ever more powerful synchrotron X-ray sources. One could thus minimize this time numerically within the constraints of the three angles α, γ and χ.

Many thanks are due to Ing. H. G. Ficke for preparing the diffractometer sketches. Professor Dr J. F. Van der Veen is acknowledged for a critical reading of the manuscript. This work is part of the research program of the Stichting voor Fundamenteel Onderzoek der Materie (FOM) and is made possible by financial support from the Nederlandse Organisatie voor Wetenschappelijk Onderzoek (NWO) and the Netherlands Technology Foundation.

APPENDIX *A*
A mirror image of the diffractometer

The calculations carried out so far only apply to one specific diffractometer set-up, in which the X-ray beam enters the sample along the positive y coordinate of the laboratory frame. In order to demonstrate how these concepts can be adapted to a different diffractometer or beam-line geometry, the necessary changes for one common example are described here.

An obvious variant of the set-up as defined above is a mirror image of the diffractometer, in which all the circles and the beam line and detector orientations are mirrored in the laboratory-frame xz plane. This mirror image is illustrated in Fig. 4. The transformation can most easily be mediated by a mirror matrix M:

$$M = \begin{bmatrix} 1 & 0 & 0 \\ 0 & -1 & 0 \\ 0 & 0 & 1 \end{bmatrix}. \tag{63}$$

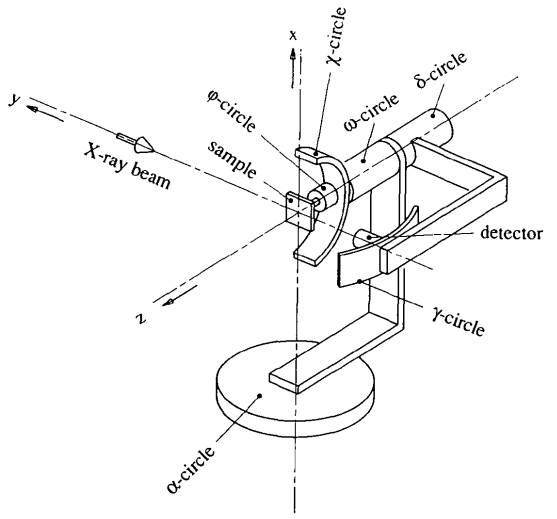

Fig. 4. Mirror image of the diffractometer. All the circles of Fig. 1 are mirrored in the xz plane.

Under the mirror transformation, the incoming- and outgoing-X-ray-beam vectors are changed:

$$\mathbf{K}_{i,\mathrm{lab}} \rightarrow \mathbf{K}'_{i,\mathrm{lab}} = M\mathbf{K}_{i,\mathrm{lab}} \tag{64a}$$

$$\mathbf{K}_{f,\mathrm{lab}} \rightarrow \mathbf{K}'_{f,\mathrm{lab}} = M\mathbf{K}_{f,\mathrm{lab}}. \tag{64b}$$

All rotation matrices, A, Δ, Γ, Ω, X and Φ [(6)], and the two orientation matrices, Σ and T [(14)], are altered according to

$$W \rightarrow W' = MWM^{-1} = MWM, \tag{65}$$

where $M = M^{-1}$ has been used. Note that neither UB nor $\mathbf{H}$ are changed.

The diffraction condition (11) then becomes

$$\begin{aligned} &M\Omega MMXMM\Phi MUB\mathbf{H} \\ &\quad = (M\Delta MM\Gamma M - MA^{-1}M)M\mathbf{K}_{i,\mathrm{lab}} \\ &\quad \Leftrightarrow \Omega X\Phi MUB\mathbf{H} \\ &\quad = (\Delta\Gamma - A^{-1})\mathbf{K}_{i,\mathrm{lab}}, \end{aligned} \tag{66}$$

where $M^2 = I$ has been used in the last step.

Correspondingly, (20) becomes

$$\sin\beta_{\mathrm{in}} + \sin\beta_{\mathrm{out}} = (1/K)(S^{-1}MUB\mathbf{H})_3. \tag{67}$$

The angle-of-incidence and outgoing-angle conditions, (15) and (16), do not change, which can easily be proved, for example, for the angle of incidence:

$$\begin{aligned} &M\Omega MMXMM\Phi MMSM\begin{bmatrix}0\\0\\1\end{bmatrix}MA^{-1}MM\begin{bmatrix}0\\1\\0\end{bmatrix} \\ &\quad = -\sin\beta_{\mathrm{in}} \\ &\quad \Leftrightarrow \Omega X\Phi S\begin{bmatrix}0\\0\\1\end{bmatrix}A^{-1}\begin{bmatrix}0\\1\\0\end{bmatrix} \\ &\quad = -\sin\beta_{\mathrm{in}}, \end{aligned} \tag{68}$$

where $M(0, 0, 1) = (0, 0, 1)$ has been used.

Similarly, the horizontal-surface-normal condition, (21), is invariant. Therefore, under the mirror transformation defined by (64) and (65), the only noninvariant term is UB. Thus, the angle calculations derived in this paper are also valid for the mirrored diffractometer, provided UB is changed into MUB.

References

Bloch, J. M. (1985). *J. Appl. Cryst.* **18**, 33–36.

Brennan, S. & Eisenberger, P. (1984). *Nucl. Instrum. Methods*, *A***222**, 164–167.

Busing, W. R. & Levy, H. A. (1967). *Acta Cryst.* **22**, 457–464.

Certified Scientific Software (1992). *SPEC*. PO Box 802168, Chicago, IL 60680, USA.

Feidenhans'l, R. (1986). PhD thesis, Risø National Laboratory, DK-4000 Roskilde, Denmark.

FEIDENHANS'L, R. (1989). *Surf. Sci. Rep.* **10**, 105–188.
FERRER, S. (1992). Personal communication.
GIBBS, D., OCKO, B. M., ZEHNER, D. M. & MOCHRIE, S. G. J. (1990). *Phys. Rev. B*, **42**, 7330–7334.
MOCHRIE, S. G. J. (1988). *J. Appl. Cryst.* **21**, 1–3.
NORRIS, C., TAYLOR, J. S. G., MOORE, P. R. & HARRIS, N. W. (1987). Daresbury Annual Report No. 124. SERC Daresbury Laboratory, Warrington WA4 4AD, England.
ROBINSON, I. K. (1988*a*). *Rev. Sci. Instrum.* **60**, 1541–1544.
ROBINSON, I. K. (1988*b*). *Aust. J. Phys.* **41**, 359–367.
STOUT, G. H. & JENSEN, L. H. (1968). *X-ray Structure Determination.* New York: Macmillan.
TAKAHASHI, T., NAKATANI, S., TAKAHASHI, M., ZHANG, X. W. & ANDO, M. (1993). *Construction of Six-Circle Surface X-ray Diffractometer.* Proceedings of IVC-12/ICSS-8, The Hague, 1992. *Surf. Sci.* In the press.
VLIEG, E., ROBINSON, I. K. & KERN, K. (1990). *Surf. Sci.* **233**, 248–254.
VLIEG, E., VAN DER VEEN, J. F., MACDONALD, J. E. & MILLER, M. (1987). *J. Appl. Cryst.* **20**, 330–337.